

# Organic ligand and solvent kinetics during the assembly of CdSe nanocrystal arrays using infrared attenuated total reflection

Bosang S. Kim,<sup>a)</sup> Luis Avila,<sup>b)</sup> Louis E. Brus,<sup>b)</sup> and Irving P. Herman<sup>a),c)</sup>

Materials Research Science and Engineering Center and the Columbia Radiation Laboratory, Columbia University, New York, New York 10027

(Received 16 February 2000; accepted for publication 19 April 2000)

The self-assembly of amorphous three-dimensional arrays of CdSe nanocrystals is probed in real time using multiple-reflection, infrared attenuated total reflection spectroscopy by following the solvent and the organic ligands that passivate the nanocrystal surface. During the self-assembly of a 250 ML array from pyridine-capped CdSe nanocrystals in pyridine solvent, the solvent molecules evaporate in  $\sim 30$ – $40$  min and the pyridine-capping molecules leave the array very slowly, apparently limited by diffusion, with  $\sim 30 \pm 8\%$  remaining after three days. © 2000 American Institute of Physics. [S0003-6951(00)00325-9]

Semiconductor nanocrystals have created great interest as possible components of complex materials because of their unusual properties, including their linear and nonlinear optical properties.<sup>1</sup> The organic molecules sometimes used to “cap” the surface of semiconductor nanocrystals can passivate surface states, stabilize dispersions of the crystallites, and form an insulating layer that electrically isolates the particles.<sup>2</sup> Three-dimensional arrays of CdSe nanocrystals have been self-assembled from solutions of these nanocrystals.<sup>3</sup> The kinetics of array formation depends on the interactions of particles with each other, the solvent, and the surface. It also depends on solvent evaporation, which is very different for monolayered arrays and very thick three-dimensional (3D) arrays; this has been little studied. Many unanswered issues also remain about the stability of organic ligands that bind weakly to the nanocrystals, such as pyridine, particularly during self-assembly.

In this letter, the density of surface ligands and solvent molecules are followed during the self-assembly of CdSe nanocrystals passivated by pyridine and tri-*n*-octylphosphine oxide (TOPO), designated as CdSe/pyridine and CdSe/TOPO, respectively, to form amorphous arrays by using multiple-reflection, horizontal attenuated total reflection (ATR) spectroscopy. ATR permits probing of (1) the loss of solvent molecules during the early stages of drying, (2) the exchange between the ligands capping the CdSe with solvent molecules, and (3) the possible desorption of these capping ligands during the later stages of drying. Since pyridine binds only weakly to the CdSe nanoparticle, mostly at surface Cd,<sup>4,5</sup> it has been thought that all of the pyridine rapidly desorbs during the formation of an array from CdSe/pyridine, leaving bare nanocrystals, at least for monolayer arrays at  $150^\circ\text{C}$ .<sup>6</sup> It is seen here that in thicker films the nanocrystals are still at least partially capped by the weakly binding pyridine, even after several days of drying.

CdSe nanocrystals 3.0 nm in diameter (with a standard

deviation of 5%) and passivated with tri-*n*-octylphosphine oxide (TOPO, CdSe/TOPO) were synthesized according to the method of Murray *et al.*<sup>7</sup> In many runs, these TOPO surface ligands were replaced by pyridine (CdSe/pyridine) by refluxing the nanocrystals in pyridine three times, each time for 3–5 h at  $60^\circ\text{C}$ ,<sup>7</sup> prior to self-assembly.

A concentrated 0.1 cc drop of capped CdSe nanocrystals in solution was placed on the top surface (7 mm $\times$ 68 mm) of the ZnSe prism, initially producing a  $\sim 210$ - $\mu\text{m}$ -thick layer. ATR spectra were taken periodically during drying, after which a disordered, amorphous array of  $\sim 0.85 \pm 0.20$   $\mu\text{m}$  thickness formed—as determined by profilometry. This corresponds to about 250 ML of CdSe nanoparticles. These measurements were performed using a ZnSe GRASEBY-SPECAC horizontal ATR accessory mounted on a PE-1000 Paragon Fourier-transform infrared (FTIR) spectrometer. Each spectrum was averaged over four scans in 16 s, and taken with a resolution of  $4\text{ cm}^{-1}$  and weak apodization. Peak heights were determined from Gaussian fits. Unless otherwise noted, all drying experiments were conducted at ambient temperature.

Figure 1 shows the ATR spectra near the  $1445.2\text{ cm}^{-1}$  peak of pyridine bound to a CdSe nanoparticle, for (1) arrays

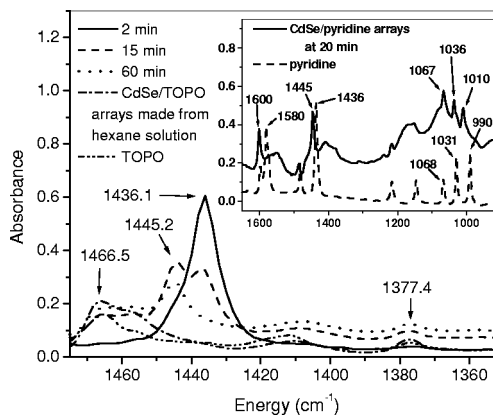


FIG. 1. ATR spectra of CdSe/pyridine arrays formed with pyridine solvent 2, 15, and 60 min into self-assembly, along with those of pure TOPO and a CdSe/TOPO array formed with hexane solution. The inset shows spectra of CdSe/pyridine arrays after 20 min and neat pyridine.

<sup>a)</sup>Also with the Department of Applied Physics.

<sup>b)</sup>Also with the Department of Chemistry.

<sup>c)</sup>Author to whom correspondence should be addressed; electronic mail: iph1@columbia.edu.

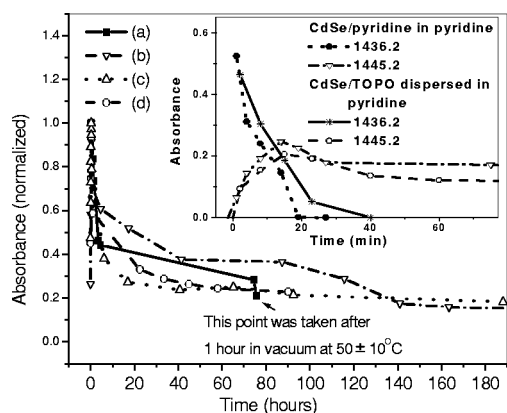


FIG. 2. Heights of  $1445\text{ cm}^{-1}$  peaks in the ATR spectra of (a), (b), (c) CdSe/pyridine arrays from pyridine solution and (d) CdSe/TOPO arrays from pyridine solution as a function of drying time, normalized to unity at the maximum of each trace. The inset shows this (unnormalized) on a finer time scale at  $1445\text{ cm}^{-1}$  (bound pyridine) and also at  $1436\text{ cm}^{-1}$  (neat pyridine).

of CdSe/pyridine nanocrystals initially in pyridine solvent dried for 2, 15, or 60 min, (2) a dried array of CdSe/TOPO nanocrystals initially in hexane, and (3) pure TOPO. This C–C, C–N stretching mode of pyridine bound to the CdSe nanocrystal at  $1445.2\text{ cm}^{-1}$  appears at  $1436.1\text{ cm}^{-1}$  in the neat pyridine. This upshift for bound pyridine is reasonable given the frequency upshift of pyridine adsorbed on Au.<sup>8</sup>

Solvent evaporation during array formation with CdSe/TOPO nanocrystals dispersed in hexane solvent was too fast to be followed with this method. No changes in the frequency or height of the TOPO peaks were observed after the hexane evaporated, showing that the TOPO remained bound to the surface; this is expected because TOPO has a very low vapor pressure. The small TOPO peaks at  $1377.4$  and  $1466.5\text{ cm}^{-1}$  in the CdSe/pyridine array suggest that even after ligand exchange with pyridine the CdSe is still partially capped by TOPO. Comparing the IR absorbances in CdSe/pyridine and CdSe/TOPO arrays,  $\sim 11\%$  of TOPO molecules remain after ligand exchange with pyridine. This is consistent with measurements of  $\sim 10\%$ – $15\%$  of the sites remaining capped by TOPO made using other methods.<sup>9,10</sup>

The spectra in Fig. 1 show that during the self-assembly the solvent peak at  $1436.1\text{ cm}^{-1}$  decreases to zero, while the pyridine-on-CdSe peak at  $1445.2\text{ cm}^{-1}$  first increases from roughly zero and then decreases. The inset in Fig. 2 follows these peaks in greater detail for CdSe/pyridine and CdSe/TOPO dispersed in pyridine. The removal of solvent in the probed region is indicated both by the decrease in  $1436.1\text{ cm}^{-1}$  peak (loss of solvent molecules) and the increase in the  $1445.2\text{ cm}^{-1}$  peak (increase of the number of nanoparticles). Complete drying of the solvent occurs in  $\sim 30$ – $40$  min. The bound pyridine peak initially increases, reaches a maximum at  $\sim 15$  min, and then slowly decreases. Since the absorbance of bound pyridine in CdSe/TOPO in pyridine traces are the same as those for CdSe/pyridine in pyridine (Fig. 2), surface exchange of TOPO for pyridine apparently occurs very fast on these time scales. (The CdSe/TOPO particles were dispersed in the pyridine solvent within  $\sim 2$  min of deposition on the ATR crystal and the first FTIR scan.) TOPO peaks still remain; a small fraction of TOPO is

still bound to the CdSe nanoparticles and most of it is interstitial and cannot evaporate.

The main part of the Fig. 2 tracks the desorption of bound pyridine to longer times, up to eight days; each trace is normalized to unity at its maximum, accounting for the optical thickness of the sample. Sample (a) was dried for 3 h under nitrogen, in vacuum for 1 h, and then under argon for 3 days—each at ambient temperature; this was followed by drying in vacuum at  $50 \pm 10^\circ\text{C}$  for an hour. In (b), (c), and (d) the samples were dried in nitrogen for 30 min and then in argon, at ambient temperature. In each case at  $20^\circ\text{C}$  there is a relatively rapid exponential decrease in absorbance with a time constant of  $\sim 208$  min, followed by a very slow decrease, with a time constant of very roughly 170 h. After three days of drying the absorbance peak decreases to  $\sim 30 \pm 8\%$  of its peak value, which means that this fraction of capping pyridine molecules remain bound. If this peak absorbance corresponds to complete surface capping by pyridine, after three days of drying  $\sim 30 \pm 8\%$  of the pyridine sites remain occupied. The rate of drying does not seem to depend on the gas environment, which is expected since there is essentially no pyridine vapor above the layer during drying (to which only  $\sim 2.1\%$  of the total surface of the nanocrystals are directly exposed). Drying at elevated temperature led to a much more rapid desorption of surface-bound pyridine.

The pyridine peaks at  $1010$ ,  $1036$ , and  $1600\text{ cm}^{-1}$  in CdSe/pyridine and  $991$ ,  $1031$ , and  $1580\text{ cm}^{-1}$  in pyridine solvent (the symmetric and asymmetric ring breathing, and C–C, C–N stretching modes, respectively<sup>8</sup>) (inset to Fig. 1) were also followed as a function of drying time. The normalized time dependences of bound and neat pyridine intensity were the same for each of these modes as for those in Fig. 2. All four modes (including that at  $1445.2\text{ cm}^{-1}$ ) were followed initially with a resolution of  $4\text{ cm}^{-1}$  and later with  $1\text{ cm}^{-1}$  resolution to look for a spectral shift of bound pyridine during drying. None was seen. In contrast, Ref. 11 reported that the  $\sim 2850$  and  $2920\text{ cm}^{-1}$  peaks of the dodecanethiol cap Ag nanocrystals in a dried array are red-shifted significantly from those of the nanoparticles in solution (by  $7\text{ cm}^{-1}$  for the latter peak).

The penetration depth in ATR is  $\lambda/2\pi(\sin^2\theta - n_2^2/n_1^2)^{1/2}$ ,<sup>12</sup> where  $\theta$  is the incident angle,  $n_{21} = n_2/n_1$ ,  $\lambda = \lambda_{\text{vacuum}}/n_1$  ( $\lambda$  is the wavelength in the prism),  $n_1$  is the refractive index of the ZnSe prism (2.4 at  $6.9\text{ }\mu\text{m}$ ), and  $n_2$  is the refractive index of the sample (1.507 at  $6.9\text{ }\mu\text{m}$  for neat pyridine).  $\theta$  is fixed at  $45^\circ$  by the prism and coupling geometry. At this angle internal reflection occurs when the external media has  $n_2 \leq 1.7$ . The beam reflects  $\sim 6$ – $7$  times from the surface covered with the array, and this does not change during drying. Right after the drop is placed on the ZnSe prism, the IR beam probes about  $0.2\lambda$  or  $\sim 1.4\text{ }\mu\text{m}$  into the solvent, and sees a very low density of nanoparticles (cumulatively  $\sim 0.7\%$  of the total). As the solvent evaporates, the density of nanoparticles in the depth probed increases, accounting for the initial increase in the bound pyridine peaks. The absorbance at the maximum of the adsorbed pyridine peak in Fig. 2 approximately equals that of the free pyridine peak, so at that time there are roughly equal quantities of bound and solvent pyridine being probed if their absorption cross sec-

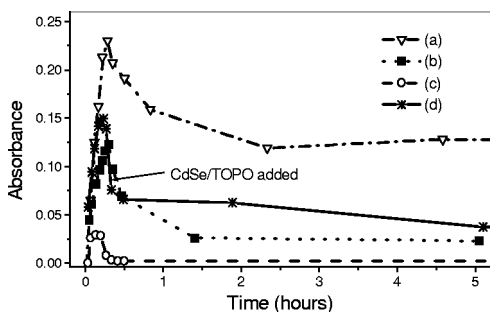


FIG. 3. Heights of  $1445\text{ cm}^{-1}$  peaks in the ATR spectra of CdSe/pyridine arrays of (a) thick  $0.85\text{ }\mu\text{m}$ , (b) thinner, and (c) thinnest arrays, and (d) array of part b covered by a CdSe/TOPO layer ( $\sim 0.1\text{ }\mu\text{m}$  thick). The fits were made to include data taken after 5 h, which are not shown.

tions are equal.<sup>13</sup> The refractive index of the array is then  $\sim 2.19$  [using effective medium theory with volume averaging of dielectric constants,  $\epsilon_{\text{CdSe}}=9.7$ , assuming face-centered-cubic (fcc) close packing of the nanocrystals with 74% packing density, with pyridine filling the interstitial regions]; it is  $\sim 2.14$  for dried arrays, with all solvent pyridine removed, 30% of the bound pyridine remaining, and unchanged interdot separations. Therefore, the penetration depth increases beyond  $1.4\text{ }\mu\text{m}$  during drying and is always  $\gg$  the maximum thickness of the dried array ( $\sim 0.85\text{ }\mu\text{m}$ ). Since  $n_{\text{array}} > 1.7$ , the infrared beam likely probes the entire depth of the dried array and is totally internally reflected at its outer surface. The total optical path (summed over all the internal reflections) does not change after the absorbance of the bound pyridine peak reaches its maximum.

Figure 3 follows the absorbance of bound pyridine for the original  $\sim 0.85\text{-}\mu\text{m}$ -thick film ("thick" array) and for films that were formed with the same volume drop with CdSe/pyridine nanocrystal concentrations that were  $\sim 1/3$  ("thinner" array,  $\sim 0.35\text{ }\mu\text{m}$  thick) and  $1/10$  ("thinnest" array,  $\sim 0.08\text{ }\mu\text{m}$  thick) as large. The thinner the film, the faster the initial decay of the bound peak pyridine peak; the time constant is 19 min for the thinner array and less than the 2 min instrumental limit for the thinnest array; it was 208 min for the thick samples. Also, the thinner the sample, the lower the long-term fractional level of bound pyridine ( $\sim 0.56, 0.19, 0.06 \times$  peak value, respectively, at 5 h). Both of these observations are consistent with diffusion out of the film with a corresponding time constant  $\propto (\text{thickness})^2$ —and not desorption—as being the rate limiting step.

Figure 3 also shows the ATR during the drying of CdSe/

pyridine in pyridine when a drop of CdSe/TOPO nanocrystals in hexane was placed on the thinner sample after the pyridine solvent had evaporated, at 17 min (see arrow). This results in an increased level of bound pyridine, presumably because the fast drying and very stable CdSe/TOPO array acts as a barrier for pyridine diffusion out of the array (as well as making the film thicker). When the diffusion barrier is applied, the rapid decrease in absorbance of bound pyridine stops, while this decrease continues in the corresponding cases with no diffusion barrier. The ATR spectra also showed increased level of TOPO in the film, which proves that the IR beam probes the entire thickness of the films, even for the thick film (not shown).

In conclusion, ATR is seen to be a quantitative real-time probe of several important features of nanocrystal self-assembly. For the self-assembled 250 ML CdSe nanocrystal arrays, the pyridine solvent evaporates in  $\sim 30\text{--}40$  min and  $\sim 30 \pm 8\%$  of the labile surface-bound pyridine molecules remain after three days. Diffusion seems to be the rate limiting step.

This work was supported primarily by the MRSEC Program of the National Science Foundation under Award No. DMR-98-09687, and also by the Joint Services Electronics Program under DAA-G55-97-1-0166. The authors would like to thank Chris B. Murray for his advice and suggestions.

<sup>1</sup>L. Brus, *Appl. Phys. A Solids Surf.* **53**, 465 (1991).

<sup>2</sup>L. R. Becerra, C. B. Murray, R. G. Griffin, and M. G. Bawendi, *J. Chem. Phys.* **100**, 3297 (1994).

<sup>3</sup>C. B. Murray, C. R. Kagan, and M. G. Bawendi, *Science* **270**, 1335 (1995).

<sup>4</sup>X. Peng, M. C. Schlamp, A. V. Kadavanich, and A. P. Alivisatos, *J. Am. Chem. Soc.* **119**, 7019 (1997).

<sup>5</sup>P. Guyot-Sionnest, M. Shim, C. Matranga, and M. Hines, *Phys. Rev. B* **60**, R2181 (1999).

<sup>6</sup>C. B. Murray, Doctoral thesis, MIT (1995).

<sup>7</sup>C. B. Murray, D. J. Norris, and M. G. Bawendi, *J. Am. Chem. Soc.* **115**, 8706 (1993).

<sup>8</sup>N. Nanbu, F. Kitamura, T. Ohsaka, and K. Tokuba, *J. Electroanal. Chem.* **470**, 136 (1999).

<sup>9</sup>M. Kuno, J. K. Lee, B. O. Dabbousi, F. V. Mikulec, and M. G. Bawendi, *J. Chem. Phys.* **106**, 9869 (1997).

<sup>10</sup>J. E. Bowen Katari, V. L. Colvin, and A. P. Alivisatos, *J. Phys. Chem.* **98**, 4109 (1994).

<sup>11</sup>B. A. Korgel, S. Fullam, S. Connolly, and D. Fitzmaurice, *J. Phys. Chem. B* **102**, 8379 (1998).

<sup>12</sup>N. J. Harrick and F. K. duPre, *Appl. Opt.* **5**, 1739 (1966).

<sup>13</sup>The IR absorption cross sections for some molecules adsorbed on metal surfaces are larger than those of free molecules, as in: S. Badilescu, P. V. Ashrit, and V.-V. Truong, *Appl. Phys. Lett.* **52**, 1551 (1988).